Subsurface Carbon Dioxide Sequestration and Storage in Methane Hydrate Reservoirs combined with Clean Methane Energy Recovery

Prashant Jadhawar [a], *Jinhai Yang* [b], *Antonin Chapoy* [b] *and Bahman Tohidi* [b]

[a]School of Engineering, University of Aberdeen, Aberdeen AB24 3UE, Scotland, UK

[b]Hydrates, Flow Assurance & Phase Equilibria Group, Institute of GeoEnergy Engineering, Heriot-Watt University, Edinburgh EH14 4AS, Scotland, UK

Abstract

CO_2 sequestration and storage into methane (CH_4) hydrate sediments is investigated in this study to evaluate CH_4 replacement by CO_2 in hydrates through both macroscale and microscale experiments at varying thermodynamic conditions. The kinetics of CO_2-CH_4 replacement in hydrates was experimentally evaluated using the production/CO_2 sequestration setup within the methane hydrate stability zone (HSZ) and within (HSZ-I)/outside the CO_2 HSZ (HSZ-II). These results were further extended at the microscale using a visual glass micromodel to validate the CH_4-replacement/CO_2 storage kinetics in presence of a commercial Kinetic Hydrate Inhibitor (KHI) to explore the feasibility of KHI for mitigation of CO_2 hydrate blockage during CO_2 injection. Up to 71% CH_4 gas recovery was obtained in the macroscale excess gas experiments within the HSZ-II, whereas the higher water saturation condition diminished this CH_4 recovery by 9.3%. Deep inside the HSZ-I, a significant CH_4 production of 51.7% was obtained (at frozen conditions) with 1% of an inhibitor application in water. For the first time ever, our novel microscale micromodel evaluations clearly revealed the release of CH_4 gas through the convection, slow CO_2 diffusive mass transfer and the CO_2-CH_4 replacement, within the HSZ-I. Moreover, this process potentially benefits from the long-term permanent CO_2 sequestration and storage in the form of clathrate hydrates while offsetting the cost of its injection through the clean energy methane recovery.

Key words: CO_2 Sequestration, Gas hydrates, CH_4, CO_2, CO_2-CH_4 replacement, Clean Energy

---

* Corresponding author: prashant.jadhawar@abdn.ac.uk (Prashant Jadhawar)

1. INTRODUCTION

Gas hydrates, also called as clathrates, are the crystalline non-stoichiometric compounds formed from the inclusion of low molecular weight gas molecules (the guests like methane, ethane, carbon dioxide, nitrogen, hydrogen, etc.) in the hydrogen bonded cage-network of water molecules (hosts), at low temperature (-10 to 25 ^{o}C) and high-pressure conditions (usually 3 to 30 MPa) in geologic systems [1, 2]. Methane hydrates are the most common hydrates found within the pores of natural sediments on the deepwater continental margins, permafrost areas and under the continental ice sheets in sediments with the global Gas-In-Place (GIP) estimates of 3000 trillion cubic meters (TCM) [3]. Their existence is confined within the Hydrate Stability Zone (HSZ) determined by the increasing geothermal gradient (1.9 ^{o}C or 275 K/100 m for permafrost and 3.2 ^{o}C or 276.35 K/100 m for oceanic) and pressure gradient in the subsurface sediments at water depths higher than 300 m in continental areas and minimum 500 m in oceanic sediments.

Estimated 30 TCM recoverable resource of methane in hydrates in sediments [4] can be produced by shifting the operational thermodynamic conditions out of the HSZ by (i) pressure reduction (depressurization) [5, 6] (ii) thermal heating: steam/hot water injection/electromagnetic heating [7, 8, 9] and (iii) inhibitor injection [9, 10] or combination of them. Except the method of depressurization that has been producing gas from natural hydrate deposits in Messoyakha of Russia, no other method has been successful in the field production [5]. Method of depressurization has been extensively applied in hydrate field production trials in Mckenzie Delta, Arctic Canada (Mallik 2002, combined with thermal method), Mallik 2007 and 2008; Nankai Trough in marine sediments (2013 and 2017), and the Shenhu area in Marine sediments (2017) [11]. The decomposition of hydrates, however, makes the grain-bindings unstable at the base of the hydrate stability zone [12], leading to landslides, serious operational hazard to offshore drilling and gas production facilities [13, 14], cause tsunamis or other natural disasters, such as the 1986 Lake Nyos disaster [15], and the methane gas release into the atmosphere seriously impacting on the global climate change [16].

Atmospheric levels of the carbon dioxide (CO_2), the major contributor (>72%) of the greenhouse gases (GHG) have been on the rise, that led to the global surface temperature increase around the world [17]. In this effort, subsurface CO_2 sequestration and geologically long-term storage scheme in methane hydrate reservoirs in the form of CO_2 hydrates was proposed by Jadhawar et. al. [18] (via kinetics and micromodel experiments). The sequestered CO_2 replaces some of the CH_4 in the hydrate crystal lattice in this novel method, converting CH_4 simple hydrates into either CO_2 hydrates or mixed CH_4-CO_2 hydrates. This process enables to (i) recover the low carbon clean energy in the form of CH_4 gas (ii) offset the cost of CO_2 transportation/compression/injection (iii) maintain the mechanical stability (seafloor integrity) of the sediments pore spaces through their reoccupation by the CO_2 or mixed CH_4-CO_2 hydrates, thus, preventing the possible slope hazards, and (iv) permanent and safe storage of the injected carbon dioxide as clathrate hydrates in subsurface geologic formations over the geologic periods, thus reducing the concentration of carbon dioxide in the atmosphere. Only one field trial has been reported for the practical application of CO_2 injection in combination with N_2 in the Ignik Sikumi area of permafrost (Prudhoe Bay, Alaska North Slope) in 2012 with some success but no solid CO_2 hydrate formation was reported during the test [19].

CO_2-CH_4 interplay in hydrates has been investigated experimentally at the molecular level using various techniques. These experiments have shown that CO_2 once in the methane hydrate reservoir, replaces some of the CH_4 in the hydrate crystal lattice, converting CH_4 simple hydrates into either CO_2 hydrates or mixed CH_4-CO_2 hydrates. CO_2 and CH_4 both form simple and mixed structure-I (sI) hydrates [20, 21]. However, the CO_2 molecule with a diameter of 5.12 Å can preferentially occupy the large cavities (diameter 5.76 Å), whereas the methane molecule, having a 4.36 Å diameter, can enter both the small and larger cavities [22]. Once CO_2 enters the cavities to form CO_2 hydrate, the 57.66 kJ/mol of heat is released in the exothermic reaction. This released heat is higher than the required heat (54.19 kJ/mol) to weaken or completely dissociate the methane hydrate structure in the endothermic reaction, thus releasing the methane gas occluded in the hydrate structure. These CO_2 hydrate formation and methane hydrate dissociation takes place according to the following reactions,

where n is the hydration number, defined as the average number of water molecules required to encage one CO_2 or CH_4 molecule. It ranges from 5.75 to 7.67 for the structure-I hydrates.

$$CO_2 + n\,(H_2O) \rightarrow CO_2 \bullet n\,(H_2O) \qquad \Delta H = (-)\ 57.66\ \text{kJ/mol}\ [23]$$

$$CH_4 \bullet n\,(H_2O) \rightarrow CH_4 + n\,(H_2O) \qquad \Delta H = (+)\ 54.19\ \text{kJ/mol}\ [24]$$

The formation and dissociation of CO_2 and CH_4 hydrates depend upon the pressure and temperature conditions within which the CO_2 injection is carried out amongst the varying hydrate stability zones (HSZ) as depicted in the Figure 1. Three distinctive regions of HSZ, indicating the thermodynamic conditions at which the CH_4 replacement in hydrates by the injected CO_2 could occur, are (i) HSZ-I: inside both the CH_4 and CO_2 HSZs [25 - 28], or (ii) HSZ-III: inside CO_2 HSZ and outside CH4 HSZ [29, 30], or (iii) HSZ-II: inside methane HSZ and outside CO_2 HSZ.

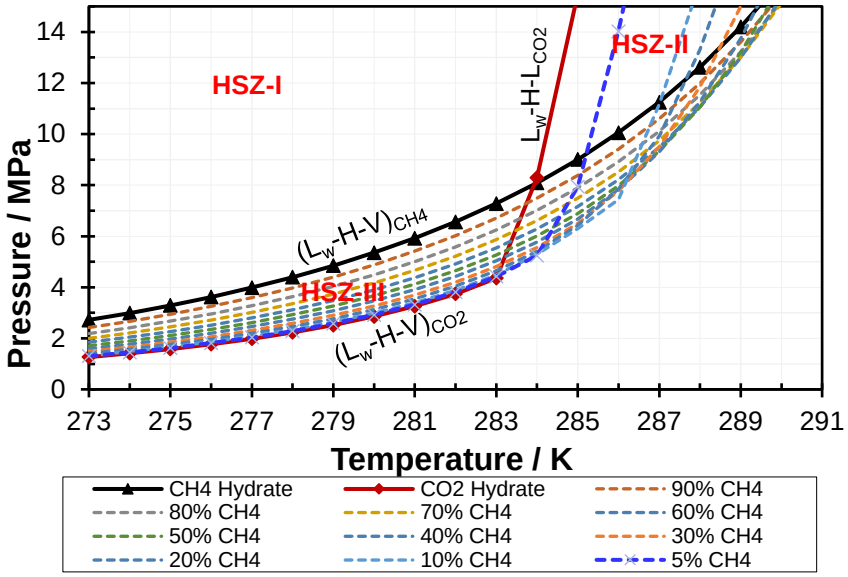

Figure 1: CH_4, CO_2 and mixed CO_2-CH_4 hydrate phase diagram indicating the three Hydrate Stability Zones (HSZ) - I, II and III (obtained through the in-house Heriot-Watt thermodynamic model [31, 32, 33])

Consequently, CH_4-CO_2 replacement mechanisms may be different when CO_2 sequestration performed in the each of the HSZs. In HSZ-III, methane in methane hydrates may be most likely replaced by CO_2

The dissociation of CH_4 hydrates may occur before the formation of the CO_2 hydrate formation or the mixed CO_2-CH_4 hydrates for the varying CO_2-CH_4 composition as displayed by the

HSZ-III in Figure-1. If the thermodynamic conditions are in HSZ-II, the CO_2 will replace CH_4 in hydrates to form pure methane hydrates or mixed CO_2-CH_4 hydrates from 5% CH4 and remaining CO2 mol% with the increasing temperature and pressure

In HSZ-I, only pure CH_4 or CO_2 hydrates can form owing to the favourable thermodynamic conditions (see Figure-1).

1.1 Studies in bulk conditions (no porous media)

Most of the experimental investigations of the methane replacement in hydrates have been performed in the bulk conditions (in absence of porous media). Ohgaki *et al.* [29, 34] first coined the concept of the selective CH_4 replacement in hydrates by the injected CO_2, thus to recover methane gas from hydrate reservoirs, to sequester CO_2 as CO_2 or CO_2-CH_4 mixed hydrates and maintain sediment stability or avoid disturbing wellbore stability. Later Hirohama *et al.* [25] also demonstrated the role of slow CO_2 mass transfer in the conversion of CH_4 into CO_2 hydrate through the CH_4 replacement rate of 0.18 mol% per day (12.5%) over 800 hours, owing to the fugacity difference between the gas phase and the hydrate phase (274–277 K and 4–5 MPa).

Microscopic kinetics of replacement using Raman spectroscopy analysis were carried out by Uchida *et al.* [35], Komai *et al.* [36], Ota *et al.* [37] and Yoon *et al.* [38]. Uchida and co-workers [35] suggested the replacement through the scrap and build mechanism of the host lattice, while the cage occupancy of guest molecules by CO_2 decreases significantly after CO_2 introduction. Komai, *et al.* [36] demonstrated the measurable replacement of CH_4 in hydrate by CO_2 within 12 hours in bulk conditions, found that their CH_4 to CO_2 hydrate conversion especially faster at the temperature range just below the melting point of ice. Ota *et al.* [27, 28] observed through laser Raman Spectroscopy that 31% of the CH_4 was recovered in 280 hours at 271.2 to 275.2 K using liquid CO2, at 3.25 MPa initial pressure. They also reported that the large cages of methane hydrates decomposed faster than the small cages, and the CO_2 replacement mainly occurred in hydrate phase (based on activation energy analysis of methane and CO_2 hydrate formation). Raman spectroscopy experiments of Yoon

et al. [38] at 278 K and 3 MPa found that the initial CH_4-CO_2 replacement rate slowed beyond the 200 min. The CO_2 hydrate formed in the outer layer was thought to be a barrier against the diffusion of CO_2, and it retarded the further dissociation of CH_4 hydrate. NMR experiments of Lee *et al.* [39] resulted in the 50% recovery of methane in hydrate in 5 hours when exposed to CO_2 gas at 270 K.

Sivaraman [26] investigated the effect of gaseous CO_2 injection on methane recovery in sand pack. McGrail *et al.* [40] found the calculated the mass transfer rates of the CO_2 penetration into methane hydrates to be slow and proposed CO_2-water micro-emulsion injection in CH4 hydrate reservoirs to supply a low-grade heat source at temperatures above the CH_4 hydrate stability zone. Lee *et al.* [41] further demonstrated this by carrying out quantitative experiments to investigate the kinetics of CO_2-CH_4 exchange by injecting liquid CO_2 into methane hydrate.

1.2 Studies in porous media

In permafrost and oceanic in-situ hydrate reservoirs, the CH_4-CO_2 replacement will be controlled by number of factors, primarily, the porosity, permeability, heat and mass transfer and secondary hydrate formation. Few recent investigations addressed some of these. Ersland *et al.* [42] reported most of the methane replacement by CO_2 in their CH_4-CO_2 replacement experiments performed on two half cylindrical sandstone cores separated with a purpose-made spacer. High specific surface areas, high permeability, good heat, and mass transfer contributed to such a fast and efficient replacement, hence the high recovery. Parshall *et al.* [43] observed that the pores were occupied that the CO_2 hydrate or CO_2-CH_4 mixed hydrate in the sediments. The coating of the methane hydrate by CO_2 hydrate shells obstructed the methane hydrate – CO_2 interactions for replacement. 35% methane recovery through the replacement mechanism from an unconsolidated sand (38.7% porosity, HSZ-II) was obtained by Yuan *et al.* [44], concluding that the higher methane hydrate saturation could also reduce the percentage of liquid CO_2 replacement.

1.3 Microscale studies

Most the experimental studies have been focussed on macroscale with an objective of obtaining the quantitative measurement of the methane recovery via various production schemes, and mechanisms/conclusions are hypothesized based on the literature findings. Critical information about the mechanisms of CH_4 replacement by CO_2 in hydrate and the subsequent methane release is a missing at microscale, especially using the visual glass micromodels. Micromodels offers a unique way of understanding these processes based on the visual observations throughout the process at the pressure and temperature conditions within the three HSZ-I, II and III.

The phase behaviour of reservoir fluids in porous media for enhanced oil recovery has extensively been studied earlier using 2D micromodels. Tohidi *et al.* [45] demonstrated their potential applications in the gas hydrate studies through the pore-scale studies on the gas hydrate growth from dissolved gas (CO_2-water), gas hydrate distribution/cementing characteristics of grains in THF-, CO_2- and CH_4-water systems. Further visual information on phase distribution in porous media reported by Anderson *et al.* [46] included the hydrate grain cementation for CH_4-water and the mixed CH_4-CO_2-water systems. Gas hydrates nucleate and grow in the water phase; presence of salts and inhibitors alter the patterns of growth and redistribution; and, the rate and patterns of hydrate formation are affected by type of inhibitors when investigated in presence of methane, CO_2 and natural gas systems. Interaction of the CH_4 gas and water, ice and CH_4 gas, CH_4 gas and CH_4 hydrate, CO_2 gas and CO_2 hydrate, liquid CO_2 and CH_4 hydrate after 30 minutes have been published later by Jang [47]. Quantitative and qualitative morphological changes during the depressurization-assisted and chemical-assisted CH_4–CO_2 replacement was investigated by Pandey *et al.* [48] using the windowed high-pressured stirred reactor.

For the first time, Jadhawar *et al.* [18] reported the visual glass micromodel observation of the occurrence of the CH_4 replacement by the injected CO_2 in hydrates replacement inferred from the formation of the mixed CH_4-CO_2 hydrates at the thermodynamic conditions where methane hydrates

are stable, but the CO_2 hydrates are unstable (HSZ-II, see Figure-1). We continue to evaluate this result in this article with the further evaluation of the role that a kinetic inhibitor plays in the CH_4-CO_2 replacement (in HSZ-I), hence the CO_2 sequestration as hydrates.

1.4 Proposed work in this study

All the reviewed experimental work so far has been carried out at different thermodynamic conditions, porosity, permeability, gas and liquid CO_2 etc. using different experimental macroscale (few) and microscale (Raman spectroscopy, NMR etc.) techniques in the bulk and porous media. However, experimental data of kinetics of the CO_2 replacement rate in the porous media are few and needs further extensive evaluation. This work aims at a better understanding of the effect of varying thermodynamic conditions of methane and CO_2 HSZ in the presence of porous media and the role of kinetic inhibitor on the CH_4-CO_2 replacement. Both the macro and microscale experimental investigations are reported in this article.

2. EXPERIMENTAL DETAILS

Tests of CH_4 replacement in hydrates by the injected CO_2 and the subsequent permanent CO_2 sequestration and storage were conducted using two experimental setups: the production/CO_2 sequestration rig and the visual glass micromodel. CO_2 injection into CH_4 hydrates in porous media in this work is aimed towards the evaluation of the macroscale (modified production/CO_2 sequestration rig) and microscale (glass micromodel) mechanisms involved in the process of CO_2 injection into methane hydrate reservoirs and consequent recovery of methane, complemented by permanent subsurface sequestration and storage of CO_2 in the form of clathrate hydrates in porous media.

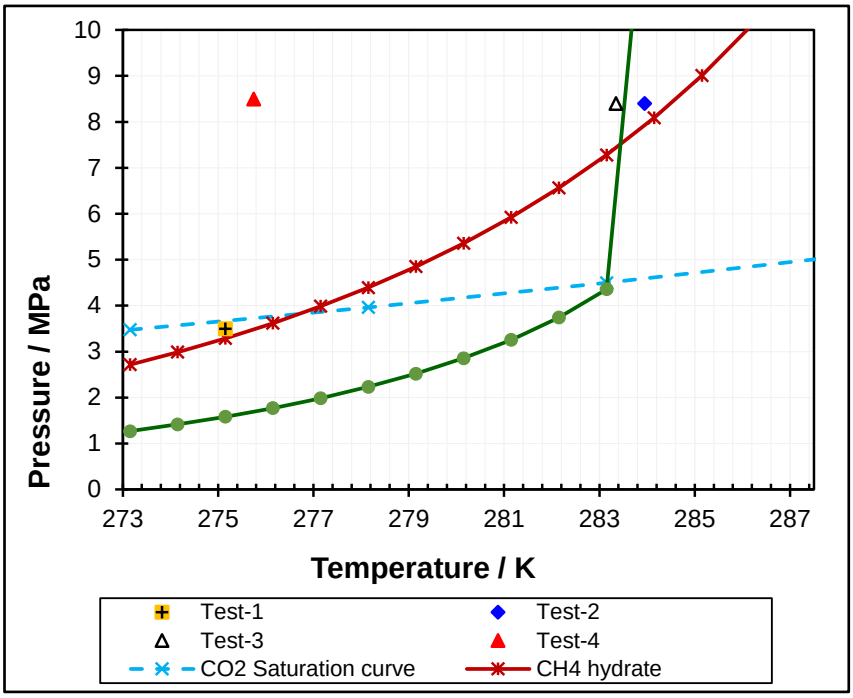

Figure 2: Methane and CO2 hydrate stability zones and the test conditions

2.1 Macroscale experiments using the production/CO_2 sequestration rig

To understand the effects of pressure and temperature conditions on the rate of the CO_2 hydrate formation and the subsequent methane release from the methane hydrates, four macroscale tests were performed on the modified CO_2 sequestration/production rig at different operating conditions as shown in Table 1 and Figure 2. All the calculation procedure for the respective parameters in Table 1 is adapted from Okwananke *et al.* [49]. These experimental investigations imitate the excess gas reservoir conditions for Tests 1, 2 and 4 (i.e. with very little or no free water such as permafrost where free gas layer overlaid by hydrate zone in permafrost hydrate deposits) and higher water reservoir conditions for Test 3 (oceanic hydrates along the continental margins). Moreover, gaseous and liquid CO_2 was injected in the Test-1 and the Tests-2, 3 and 4, respectively. An application of kinetic inhibitors (Low Dosage Hydrate Inhibitor, LDHI) was also investigated in the Test-4 to evaluate its effect on the CO_2-CH_4 replacement process.

Table 1: Test Conditions before the introduction of CO_2 in the porous media containing methane hydrates.

Test	Temperature	Pressure	Saturations (vol%)			Porosity	
	(K)	(MPa)	Hydrate (Sh)	Gas (Sg)	Water (Sw)	(fraction)	Test details
1	275.2	3.6	22.4	75.7	1.97	50	Excess Gas, Gas CO_2 injection
2	284	8.4	21.9	74.8	3.4	39	Excess Gas, liquid CO_2 injection
3	283.4	8.4	33.7	39.6	26.7	44.7	Higher water saturation, liquid CO_2 injection
4	275.8	8.5	51.3	37.3	11.3	50	Higher hydrate saturation, liquid CO_2 injection, the effect of KHI

2.1.1 Materials

Glass beads of 0.5 mm diameter purchased from BioSpec Products Inc. to act as a reservoir sediment to simulate the porous medium. CH_4 and CO_2 gases were purchased from Air Products PLC, with a certified purity 99.995 vol. %. Distilled water was used in all the experiments to partially saturate the glass beads. A kinetic hydrate inhibitor, LuviCap, was supplied by CLARIANT.

2.1.2 The experimental setup

Figure 3 shows the schematic view of the production/CO_2 sequestration set-up. It consists of a high-pressure piston cell made of 316 stainless-steel with maximum pressure rating of 40 MPa and maximum working volume of 627 cm^3 (Cell dimensions: 14.1 cm height and 7.5 cm diameter), a feed system for CH_4, CO_2 and water, and instrumentation for measuring temperature and pressure. The test cell has two endcaps: One is fixed, and the other movable is driven by hydraulic fluid (water). The pore pressure is maintained by applying a constant hydraulic fluid pressure (overburden) behind the movable piston. Using a piston system sediment could be compacted at any given overburden pressure. A displacement meter (Linear Variable Differential Transformer – LVDT) fitted to the steel rod tail determines the piston position, hence the exact volume of the cell. Pore fluid pressure is controlled independently. A coolant jacket with circulating fluids surrounding the test cell is controlled by a programmable cryostat (253 K to 353 K) and can be kept stable to within ± 0.05 K. Temperature and pressures are monitored through a Platinum Resistance Thermometer (PRT) and

Quartzdyne pressure transducers (accuracy of ± 0.008 MPa for 0-138 MPa), respectively. A syringe pump is used to inject the test fluids in the cell through piston vessels. The overburden pressure was measured by a Druck pressure transducer with an accuracy of 0.05 MPa connected to the back of the piston. LabView software interface (National Instruments) monitored and recorded the cell pressure, temperature, overburden pressure, and piston displacement on a computer at 60s interval via a Data Acquisition System from National Instruments. Measurement of the gas compositions during CO_2-CH_4 replacement experiments was carried using a gas chromatograph (VARIAN model CP-3800).

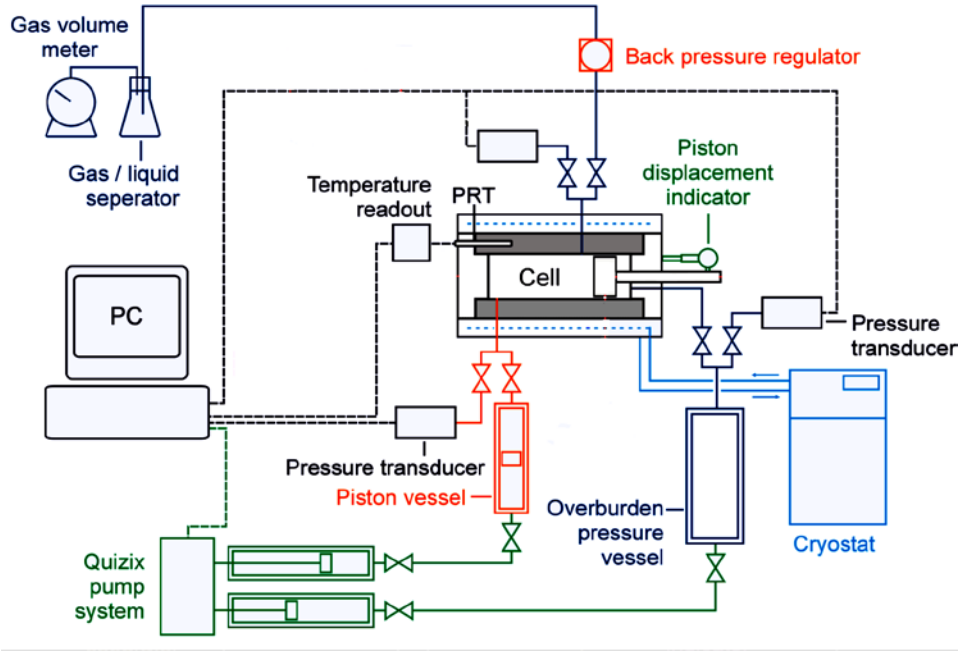

Figure 3: Experimental set-up for CO_2 sequestration tests

2.1.3 Experimental Procedure

Four experimental tests were conducted under excess gas and excess water conditions, in three steps viz. methane hydrates formation, injection of carbon dioxide in the methane hydrate-vapour system, and finally, the measurement of methane recovery and CO_2 sequestered and storage. Pressure and temperature conditions for the Test-1 (3.6 MPa, 275.2 K) and Test-4 (8.5 MPa, 275.8 K) were set inside the HSZ-I of both the methane and CO_2 hydrates. Most of the water and methane was utilized for the methane hydrate formation i.e. under excess gas conditions while maintaining the

pressure below the CO_2 saturation pressure. Test 2 was conducted at 8.4 MPa and higher temperature 284 K falling in the HSZ-II. Test 3 was conducted at the same pressure and 283.4 K inside the HSZ of the methane hydrate and just inside the CO_2 hydrate equilibrium condition (HSZ-I). Figure 2 shows the thermodynamic conditions and the hydrate phase boundaries for the methane and CO_2 hydrates obtained through the in-house Heriot-Watt thermodynamic model .

Methane Hydrate Formation: In Test 1, the glass beads were charged into the cell to occupy 50% of the total cell volume, and saturated with water. In Tests-2 and 4, the cell was not completely filled with the sediments and there was a small free space at the top of the cell, while in Test-3 the cell was completely filled with the sediments. After removing air through vacuum, overburden pressure was applied, and methane gas was injected into the cell at room temperature until the system pressure reached the pressure higher than the three-phase equilibrium pressure of CH_4 hydrate and then allowed to reach phase equilibrium. Then the system was cooled down to 273.7 K to form methane hydrates. The test cell pressure continued to decrease for a number of hours during the initial stages of cooling, which then dropped sharply as the methane hydrate begins to form, indicating that the methane molecules being occluded in hydrates. Growth of methane hydrates was continued even before the injection of CO_2 into the cell. The quantities of the injected water and methane were measured for determination of hydrate saturation.

CO_2 injection: The temperature of the test cell containing the newly formed methane hydrate was reset to a target temperature for the CO_2-CH_4 replacement investigation. Methane gas was withdrawn from the top to reduce the cell pressure, ensuring it to be above the CH_4 HSZ and then CO_2 was injected through the inlet at the bottom of the cell. This CH4 withdrawal and CO2 injection cycle is repeated in few cycles until the methane concentration in the top of the cell (gas phase) is lowered to the desired acceptable level. The target pore pressure was achieved by controlling the volume of CO_2 injection.

After testing and validation of the miscibility of the LDHI in the liquid CO_2, the LDHI in liquid CO_2 mixture was injected in the test rig using a piston cylinder in Test-4. The pressure of the

CO_2 cylinder while it is injection into a piston vessel is kept higher than the CO_2 saturation pressure, normally 8.27 to 10.34 MPa. The pressure inside the system was kept above the three-phase equilibrium pressure of methane hydrate.

Methane recovery: The system pressure is reset to the target conditions and the methane hydrates along with some free water are allowed to soak with the CO_2-CH_4 gas mixture for a certain period while maintaining the constant overburden pressure (hence the pore pressure) using a Quizix pump. For each equilibrium condition, 10 ml gas samples are withdrawn from the sampling port in every 24 to 72 hours, and then swept to a Varian 3800 gas chromatograph for analysis. As the volume of the withdrawn samples was very small compared to the total volume of the equilibrium cell, it was assumed that the sample withdrawals did not have any significant effect on the phase equilibria. Table 1 shows the experimental conditions for CO_2 replacement in this study.

2.2 Microscale experiments using a visual glass micromodel

In this study, the visual observations of the pore-scale mechanistic evaluations of the CH_4-CO_2 replacement and the potential for the underground storage of the sequestered carbon dioxide especially in methane hydrate reservoirs is investigated using the visual glass micromodel. Results of the experiments conducted on the medium pressure micromodel provide an insight into an effect of a kinetic inhibitor on the CH_4-CO_2 replacement process in methane hydrates upon the CO_2 injection in the already existing methane hydrates in porous media.

2.2.1 Materials

Methane and carbon dioxide gas were obtained from Air Products PLC, with a certified purity 99.995 vol %. Distilled water used in these micromodel experiments. Methyl blue dye to mix with the distilled water and observe the contrast between the methane hydrates and injected CO_2. Luvicap, a kinetic inhibitor was supplied by a Clariant. Two small piston vessels of volume 10 cubic

centimetres, pressure rating 41.36 MPa were employed for the injection of the methane and carbon dioxide gas.

2.2.2 Test Apparatus for the Visual Micromodel Experimental Investigation

Glass micromodels have been employed in studying a wide range of hydrate systems from hydrates in subsea sediments to flow assurance to obtain novel visual information on the mechanisms of clathrate growth, dissociation and phase distribution at the micro-scale, with respect to pressure, temperature, wettability and fluid composition [40]. A medium pressure glass micromodel (8.3 MPa) used in this study that consist of an etched glass base-plate topped with a sealed glass cover plate as represented. Either a geometrically designed network of pores, tubes, or reproductions of actual thin sections of real sediments, can be used to construct the micromodels by etching with hydrofluoric acid. The cover plate has an inlet and outlet, which allows fluids to be pumped through the enclosed pore network using small-volume piston vessels or a precision *Quizix* pump (refer to Figure 4).

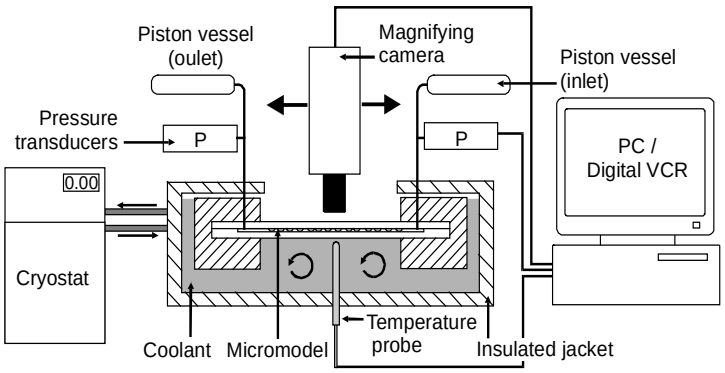

Figure 4: Experimental set-up of a medium pressure glass micromodel [18]

Glass micromodels are mounted in a vessel that exerts an overburden pressure and is surrounded by coolant jackets controlled by the temperature-controlled baths. Temperature is measured by a probe mounted in the overburden cell, and transducers measure pressure on the model inlet and outlet lines. Temperature can be kept stable to within ± 0.05 K. Temperature and pressures are monitored through a PRT and *Quartzdyne* pressure transducers (accuracy of ± 0.008 MPa for 0-138 MPa), respectively. Magnifying cameras are mounted above the micromodel, with illumination

being provided by cold light sources. Because the micromodel pores structure is only one pore thickness deep, it is possible to observe phase changes and fluid flow behaviour inside the micromodel. The selective pictures represented here are the one recorded either from video footage or camera clippings.

2.2.3 Experimental procedure

Two glass micromodel experiments are conducted through the steps of methane hydrates formation and then the CO_2 injection in the methane hydrate-water system without or with the injection of a low dosage kinetic inhibitor (LDHI) in the micromodel pores network. In practice, the subsurface CO_2 injection faced with the formation of hydrate around the wellbore, thus obstructing the further advance of the injected CO_2 in the methane hydrate formation pay zone. In order to find solution to this practical issue, we experimentally evaluated an application of 1 mass% LuviCap LDHI inhibitor in water solution to delay the blockage of the near-wellbore zone of the CO_2 injection well, thus allow the further advance of the injected liquid CO_2 to contact the methane hydrates for the intended CH_4-CO_2 replacement and the methane recovery.

In the micromodel experiments, the distilled water dyed with methyl blue (0.7 mass%) is used as an experimental fluid. Hydrates and gas exclude this dye, thus increasing the contrast between the phases, while it is not known to have any measurable effect on clathrate stability. An experimental fluid was then charged into a piston vessel and vacuumed for approximately 3-4 minutes to remove any trapped air, which is then injected into the micromodel thought the inlet valve. Methane gas was then injected in the micromodel pores 100% saturated with the dyed water using a cylinder vessel (200 cm^3 and 9.31 MPa capacity), the pressure of which was kept about 1.4 MPa higher than the outlet pressure and 0.7 MPa lower than the overburden pressure. Initial temperature, the outlet and overburden pressure of the system was noted at this stage. The pressure inside the micromodel system continues to rise gradually. Once the inlet pressure nearly equals the outlet pressure, the outlet valve was slowly opened to discharge some experimental fluid and to allow the methane gas to enter the

system. Once it was also ensured that sufficient volume of water is available for the methane hydrates to form the inlet valve was closed and system fluids (water and methane) are set to achieve the equilibrium.

The system temperature was then set to the target experimental pressure and temperature conditions. Enclathratization of the methane gas starts inside the water host structure within the two to three hours. This process of the hydrate nucleation to the full hydrate formation was completed in 5 hours to 12 hours respectively when all the methane gas diffuses through the hydrate layer and there is no further hydrate formation. To investigate the CO_2-CH_4 replacement and the subsequent CO_2 sequestration, the liquid CO_2 is injected into methane hydrates-water system inside the micromodels using a pressurised piston cylinder. Subsequent changes in the CH_4 hydrate-water-Liquid CO_2 are monitored continuously through the capture of video recording and still images, which were analysed.

To evaluate the effect of LDHI in the second micromodel experiment, the mixture of LDHI dissolved in methane saturated water was charged into methane hydrate-water system of the micromodel using a piston-cylinder. Once entry of LDHI into micromodel system indicated by the appearance of colourless liquid sufficiently spread throughout (visually observation), the valve is stopped. The stage is then set for the injection of liquid CO_2 in the micromodel. This step was then followed the CO_2 injection procedure as described above.

3. EXPERIMENTAL RESULTS AND DISCUSSIONS

Four macroscale experiments on the modified production / CO_2 sequestration rig were performed at the varying thermodynamic conditions (refer to Table 1) to investigate the CH_4 recovery from gas hydrate through its replacement by the gas (Test-1) and liquid CO_2 (Test-2 through Test-4) using the glass beads representing the porous media. Values of hydrate, gas and water saturations and the porosity after the methane hydrate formation step in each of those experiments are also presented in Table 1. Calculation procedure is adapted from Okwananke et al. [49]. Two experiments on the

visual glass micromodel further represents the microscale evaluation of mechanisms leads to the CO_2-CH_4 replacement and simultaneous CO_2 sequestration and storage in the form of hydrates in porous media.

3.1 CO_2-CH_4 replacement in gas hydrate reservoirs and CO_2 storage evaluation using the modified production / CO_2 sequestration rig

Test-1 was carried out through the gaseous CO_2 injection at the thermodynamic conditions inside both the CH_4 and CO_2 HSZs. After methane hydrate formation there was no extra water injected. Upon injection, CO_2 starts to replace methane in hydrates at the first layer at the gas CO_2-methane hydrate interface, providing the recovery of 1.27 mol% of methane within the first 17 hours (see Figure 5). Moreover, the injected CO_2 having higher solubility in the available free water (2%), could have formed the CO_2 hydrate as thermodynamic conditions are within the hydrate stability zone of CO_2 hydrates. As the heat of formation of CO_2 hydrate higher than the one required for methane hydrate dissociation, the sensible heat generated could have weakened or disrupted the hydrogen-bonded network of hydrate crystal lattice structure to dissociate the layer/s of existing methane hydrate in its vicinity. This liberates methane gas from hydrate structure into the gas phase (headspace) to further increase the headspace methane concentration.

Methane hydrates that have not been covered with free water start interacting immediately with the injected CO_2. As hydrates formed around the wetting porous media sediments (glass beads), the path of the injected CO_2 gas would be tortuous to contact these CH_4 hydrate sediments. The two processes, mainly CO_2 hydrate formation from the available free water and the interaction of the injected CO_2 gas with CH_4 hydrates, occur concurrently. Hence the simultaneous enclathratization of both CH_4 and CO_2 in the hydrate structure from CO_2 in the headspace gas is possible. However, carbon dioxide would selectively occlude in the large cavities rather than the small cavities [50]. As CO_2 molecule diameter has the same size to fit into a large hydrate cavity while CH_4 gas molecules would occupy the small cavities. Thus, most of the free water could be utilized for CO_2 hydrate

formation. It is more likely that the rate of CO_2 going into the hydrated state would be higher than CH_4 thus driving further methane displacement at this stage. Mixed CH_4-CO_2 hydrates possibly formed at this stage, which might have slowed down the exchange during the latter stage. A small decrease in system pressure was also observed during this period, and no rise in temperature was observed (which could be due to the large heat capacity of the system).

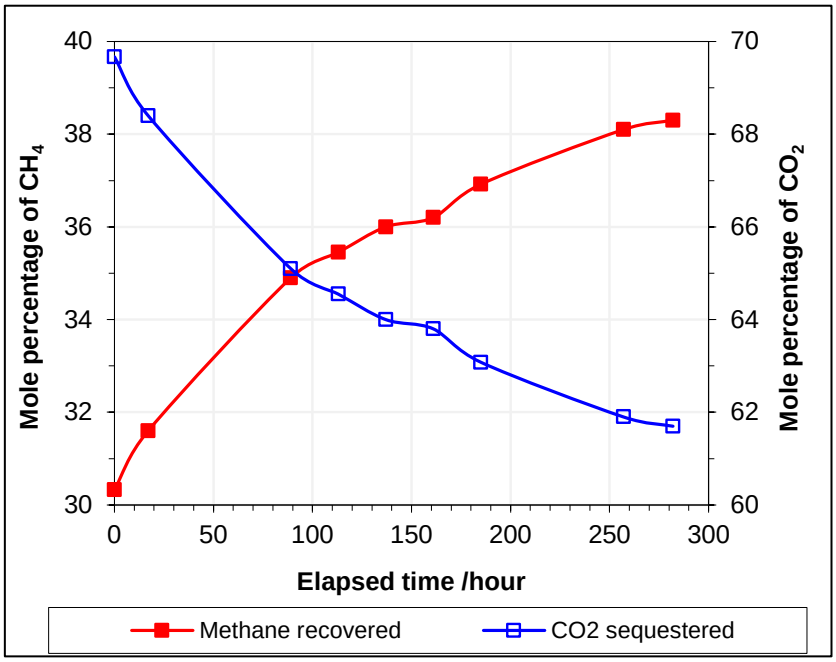

Figure 5: Methane recovery while sequestering gas CO_2 in Test-1, inside Hydrate Stability Zone (HSZ) of both CH_4 and CO_2 hydrates. Excess gas condition. Average CH_4 recovery rate: 0.77 mol% per day.

Further displacement of CH_4 in hydrate structure by the occlusion of injected CO_2 could only be due to the mass transfer of headspace gas by slow diffusion mechanism. An interface between the headspace gas and the converted mixed CH_4-CO_2 hydrates in the porous medium may not form the uniform and continuous hydrate film (as less free water was available before CO_2 injection), thus there could be available channels through which the solute CO_2 gas can be transported to the inner layer of methane hydrate sediments to continue further methane displacement. Slow diffusive mass transfer of CO_2 through the porous sediments drove further methane replacement to recover additional 3.3 mole% of methane in the next 72 hours. Methane recovery consistently continued to increase with the recovery of 0.70% mole per day for about 10 days until the termination of the experiment.

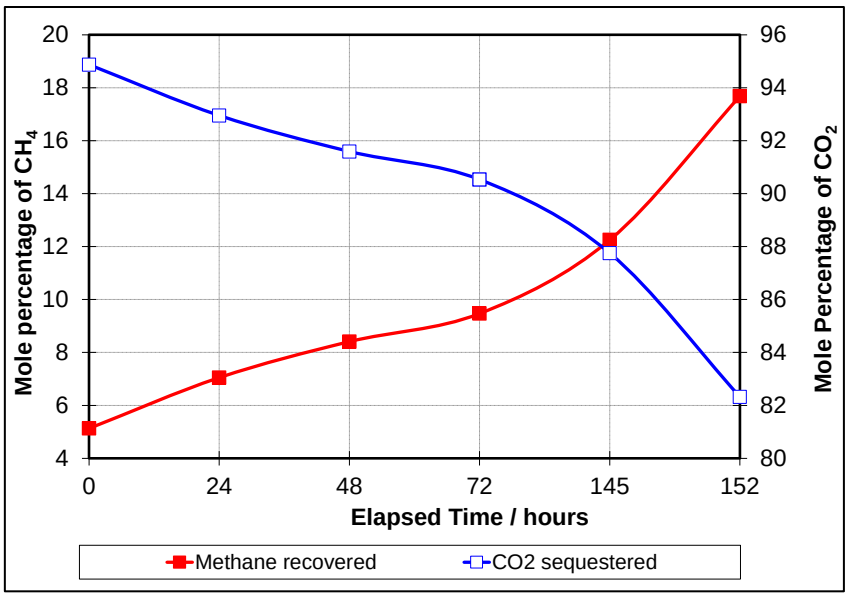

Figure 6: Methane recovery while sequestering Liquid CO_2 in Test-2, inside HSZ of CH_4 hydrates, but outside HSZ of CO_2 hydrates. Excess gas conditions. Average CH_4 recovery rate: 1.98 mol% / day.

Liquid CO_2 was injected in Test-2 at pressure (8.4 MPa) and temperature (284 K) conditions such that the CO_2 alone cannot form hydrates. Injected liquid CO_2 starts interacting with the available water (3.4%) and methane hydrate (about 22%) immediately. As CO_2 has a higher solubility than methane gas it goes into free water and the mixed CO_2-CH_4 hydrate formation occurs from the dissolved CO_2. This leads to the evolution of heat to weaken/disrupt hydrate bonded network of methane hydrate crystals liberating methane gas. Simultaneously the liquid CO_2 in direct contact with methane hydrates drive displacement of methane in hydrate structures via slow diffusion mechanism across the hydrate-liquid CO2 interface. The cumulative result is that the methane concentration is increased. In the first 72 hours, 4.36 mol% methane was recovered, 1.1 mol% higher than the Test-1 (3.3 mol%), which further increased by 8.21 mol% in the next 80 hours (refer to Figure 6). 12.55 mole % of methane were recovered in 152 hours with a recovery rate of about 2 (1.98) mole% per day. This is the novel experimental determination of CH_4 recovery through its displacement in hydrate structures by the injected CO_2 at the thermodynamic conditions outside the CO_2 HSZ. More than double methane recovery rate was observed in this test compared to Test-1. Moreover, these replacement/recovery rates of 0.68 mole% per day and 1.98 mole% per day in porous media were

high compared to the results published by earlier researchers (in the absence of porous media). Hiroshima and his co-workers (1996) recovered 6.9 mole% of methane in the gas phase over 800 hours (0.21 mole% per day) when CO_2 was used to replace methane in hydrates in the presence of a methane hydrate-water system (absence of porous media i.e. bulk conditions).

In Test-3, 26.7 mol% water was prevalent in the methane hydrate-water system in the test cell just before the liquid CO_2 injection, mimicking the seafloor hydrates. Pressure and temperature condition, 283.4 K and 8.4 MPa respectively, falls just inside both the CO_2 and CH_4 HSZ. As depicted in Figure 7, the initial compositions of CH_4 and CO_2 were 1.29 and 98.71 respectively, meaning that most of the methane was consumed into the hydrate formation before liquid CO_2 injection. In 50 hours, CO_2 concentration declined by 0.25 mol%, indicating that some of the free CO_2 molecules occluded in the hydrate structure and others solubilize in the water being significantly higher soluble compared to CH_4. This could be the induction period for the CO_2 hydrates formation, which may lead to the heat evolution weakening hydrogen-bonded network of methane hydrates that are in the vicinity of the just-formed CO_2 hydrate layer. Thus, releasing the methane molecules from hydrate cavities leading to 0.15 mol% methane recovery. CO_2 and methane hydrate formation continued. However, the rate of methane hydrate formation may be higher in the next 24 hours. Further process of CO_2 occluding the hydrate cavities was more pronounced yielding higher methane recovery over the next 34 hours through the CO_2-CH_4 replacement. Further analysis of gas samples indicated that formation of both methane and CO_2 hydrates continued for longer periods. 0.77% methane was recovered through replacement with CO_2 in hydrates whereas while storing the CO_2 in the porous media as hydrates. Beyond this stage, the methane recovery rate increased to recover 1.28% in 48 hours. The cumulative recovery was observed to be 0.17 moles% per day in this test. Particularly this test included a higher saturation of free water.

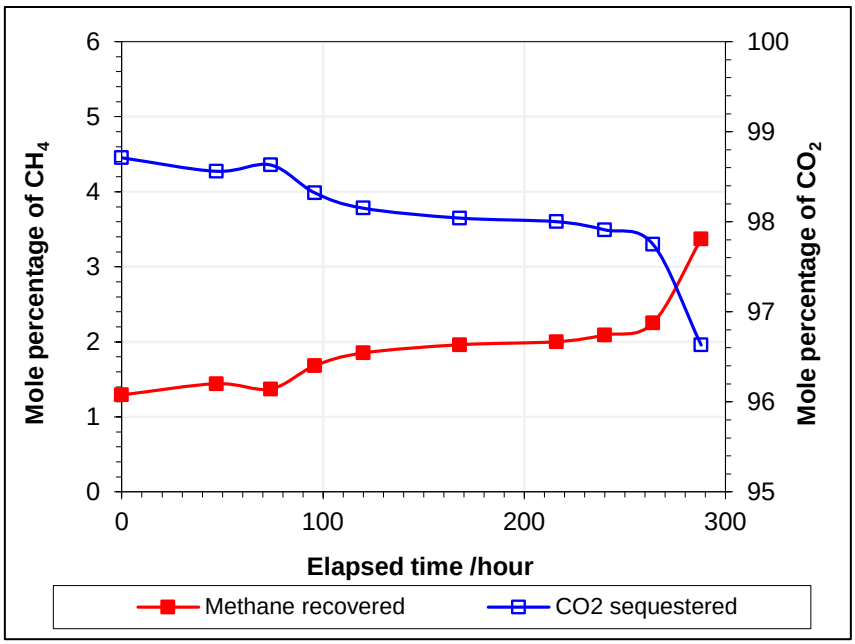

Figure 7: CH_4 recovery while sequestering liq. CO_2 in Test-3, inside CH_4 &CO_2 hydrates HSZ. Average CH_4 recovery rate: 0.17 mol%/day.

Upon the introduction of CO_2, hydrate nucleation starts either from the dissolved carbon dioxide in the water (being highly soluble in the water) or at the water liquid CO_2 interface layer. Hydrate nucleation could have begun at the water and liquid CO_2 interface layer, with CO_2 hydrate growth further inside in the water phase from the interface. The dissolved CO_2 is transported from the liquid CO_2 phase to water across the interface. Amount of heat generated from CO_2 hydrate formation will be transported towards the rock matrix and the methane hydrates. As the system also contains methane hydrates, the effect is that the heat evolved from CO_2 hydrate formation will be sufficient to weaken the hydrogen-bonded network of methane hydrate structure to release methane. At the given thermodynamic conditions, CO_2 is in a liquid state and released methane would be in gaseous state (gravity difference). Hence the released methane can be produced from the production well. The available free water may also induce the formation of pure methane hydrate (to a lesser extent due to decreased water saturation and higher CO_2 affinity towards large hydrate cavities) or mixed hydrates of the existing CO_2 and methane. Since the free water saturation decreases with the continuation of CO_2 hydrate formation or mixed CO_2-CH_4 hydrate formation for about 240 hours of

the first phase of the experiment, the further methane recovery by CO_2 displacement in hydrate structures comes from the pronounced diffusion-controlled process.

It is also possible that hydrate film [51] of pure CO_2 and / or mixed CO_2-CH_4 hydrate could be formed around the existing methane hydrates. However, its thickness will not be uniform in a microscopic sense. Film thickness can vary depending on the magnitude of the thermodynamic driving force, transport of heat and the solute CO_2, the number of original nucleation sites, type of the sediments, degree of hydrate dispersion in sediments (glass beads in this test), gas transport and the crystal morphology. Despite the formation of hydrate film, CO_2 will be transported across the film through a diffusion mechanism. However, the formation of such hydrate film possibly further slows down the CO_2 diffusion across the film. Formation of hydrates deeper inside the sediments irrespective of the existence of hydrate film is supported by the test conducted by Sivaraman [26]. Additionally, there would exist the thin sections of hydrate film that may eventually break to provide the chances of growth of massive hydrate growth across the film [5]. However, the transport rate of the solute CO_2 across hydrate film would slower than the CO_2 transport across the water-CO_2 interface towards the water phase [52].

In natural gas hydrates, liquid water film separates the methane hydrates from the mineral (rock matrix) surfaces, providing channels for the transport of the hydrate former. As significant 26.7 mol% of free water is existing in the current test, such channels could be prevalent to further aid methane replacement in hydrates by the transport of CO_2. Additionally, the presence of reservoir heterogeneities in the form of fractures and permeability variations can also positively influence the CO_2 induced methane displacement in hydrate layers.

Furthermore, CO_2 can occupy larger cavities than methane. Because the molecular diameter of CO_2 and hydrate cavity (5^{12}) diameter being nearly the same [1], methane occupies smaller cavities and a comparatively lesser fraction of the cavities available for the hydrate formation. As much as

64% of methane can be recovered from hydrate cavities for the hydrates having hydrate number of 6.0 [39].

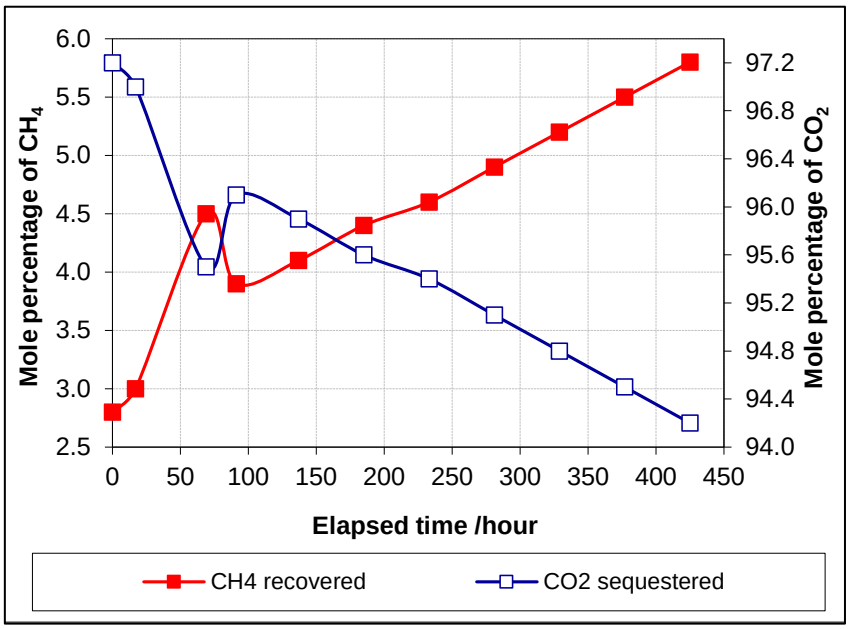

Figure 8: Methane recovery while sequestering Liquid CO_2 in Test-4, inside the methane and CO_2 hydrate HSZ. Average CH_4 recovery rate=0.17 mol% / day. Excess water conditions, Application of PVCap inhibitors.

A kinetic inhibitor LuviCap was employed in Test-4 to investigate whether it can help the injected liquid CO_2 to contact the methane hydrates in porous media deep inside the interface and thus increase the CO_2-CH_4 replacement. The idea was to delay the CO_2 hydrate formation immediately upon the CO_2-water contact as thermodynamic conditions are within the HSZ of both he methane and CO_2 hydrates if the slug/s of chemical inhibitor/s are injected before the liquid CO_2 flooding. 78.57cc of LuviCap was injected before CO_2 flooding step in this test. Saturations of methane hydrate, free gas and free water before the CO_2 injection were 51.3%, 37.3% and 11.3% respectively.

In the first stage of this test, CO_2 does start to interact with methane hydrates upon its introduction. With the presence of LuviCap, the onset of CO_2 hydrate formation was expected to be delayed. Eventually the injected CO_2, then directly encounters methane hydrate, thereby weakening of hydrogen bonding and van der Waal forces, thus diffusing through to replace methane in hydrate

cavities. Compositional changes represented in Figure 8 shows that 1.7 mole% of the methane was replaced by the injected CO_2 in the initial 69 hours (0.6 mole%/day), which is higher as compared to the results of methane replacement tests in the absence of inhibitor (nearly 0.1 mole% in 70 hours in the absence of hydrate inhibitor (Test-3, see Figure 8). As the test proceeds further, the LuviCap effectiveness reduces, the released methane from the hydrates and free CO_2 could have started to form hydrates with the available water. In the next 334 hours, about 2 mole% of methane was recovered with 0.14 mole% per day. This indicates that the rate of displacement in presence of kinetic inhibitor is higher (0.6% per day) especially until the onset of CO_2 hydrate crystals (due to the delaying action of LuviCap). Moreover, it has also been found that with the formation of the so-called hydrate (CO_2 or mixed methane-CO_2) film, that prevents the direct contact of methane hydrate with the liquid CO_2, the rate of methane replacement by CO_2 further diminishes. It is found to be slower (0.14% per day) compared to the replacement occurred in the first 69 hours. This test is a unique and first ever example to evaluate an application of a kinetic inhibitor in the CO_2-CH_4 replacement in hydrates and the subsequent CO_2 sequestration and storage option.

3.2 CO_2-CH_4 replacements and CO_2 storage evaluation using the visual glass micromodel

To mechanistically evaluate the macroscale results of the Test-1 through Test-4 conducted using the modified production/CO_2 sequestration rig, a microscale micromodel test (Test-1) was conducted to understand the microscopic mechanisms of the CO_2-CH_4 replacement and the CO_2 trapping in gas hydrates under excess water condition. Moreover, the conclusions derived from the macroscale Test-4 were further tested in the second micromodel test for the microscale evaluation of the effect of LuviCap inhibitor on the CO_2-CH_4 replacements and CO_2 storage.

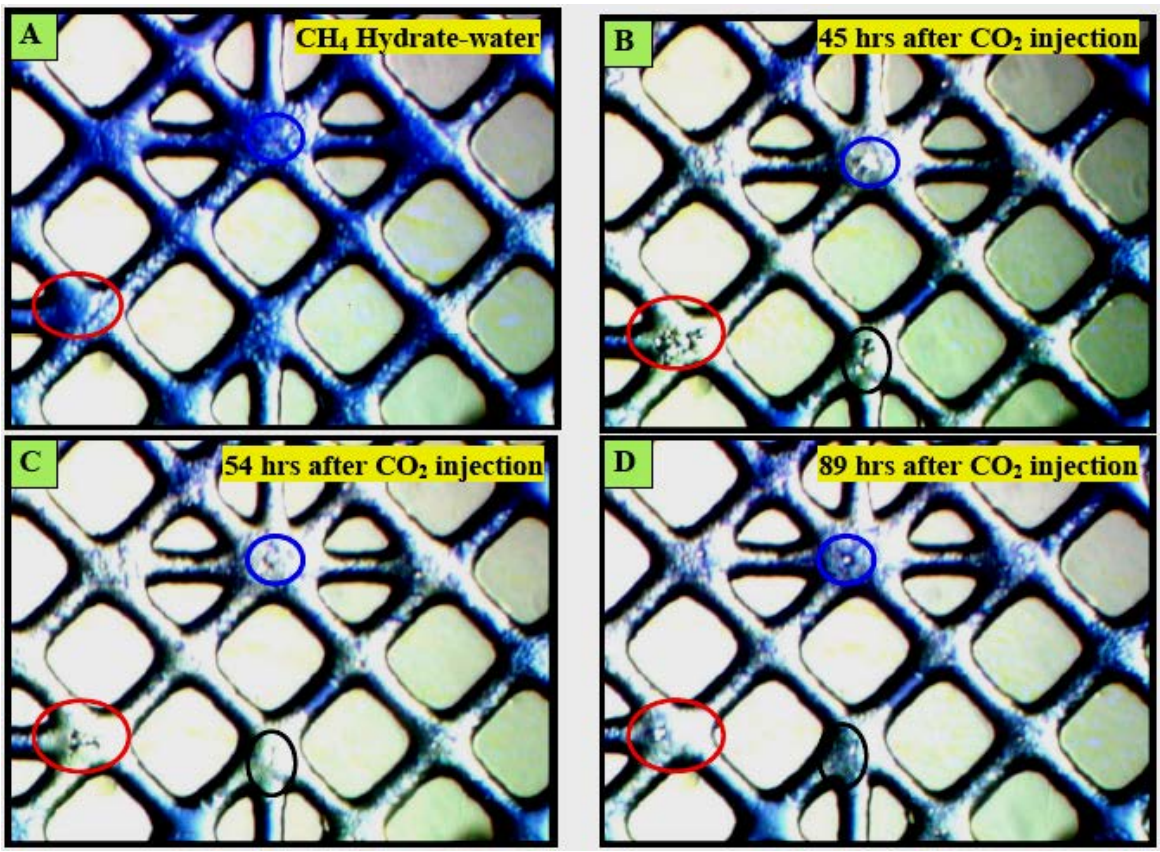

Figure 9: visual micromodel observations of methane hydrates formation (Figure A) and then subsequent changes in the already existing Methane Hydrates morphology following the CO_2 injection. Formation of the CO_2 and /or mixed CO_2-CH_4 hydrates is clearly observed (modified from Jadhawar et al., 2006)

Test-1 was conducted in the simple methane hydrate - water system simulating the excess free water conditions under the naturally occurring oceanic hydrate rich sediments. Pressure and temperature conditions were inside the CH_4 HSZ, but outside the CO_2 HSZ (284 K to 284.85 K, 8.273 MPa), and CO_2 is in a liquid state (HSZ-II, see figure 9). It has been observed that the methane hydrates existed in Figure 9A changed its morphology 45 minutes after the CO_2 injection as displayed in Figure 9B. This indicates that the injected CO_2 could have begun to form its hydrates from the free or dissolved CO_2. Generation of localized sensible heat from CO_2 hydrate formation might have dissociated some of the methane hydrate in the vicinity of the CO_2 hydrates, to release methane in hydrates. But the released methane encounters water immediately. Since the pressure and temperature conditions are conducive for the hydrate formation, methane or mixed CH_4-CO_2 hydrates might have formed at this stage. Mixed hydrate formation has been verified by the continuation of hydrate formation when system was subjected at higher temperature and pressure of 284.15 K and 9.6 MPa

respectively, to observe changes in the morphology. At these conditions, only two hydrates are stable, either methane or mixed CH_4-CO_2 hydrates.

Hereafter methane in hydrate structures in other locations/sections of micromodel could have been replaced by CO_2 molecules slowly diffusing through the formed hydrate layers. Carbon dioxide surrounding the CH_4 hydrate crystals displaced methane (weakening of hydrogen bonds to destabilize the hydrate structure), which can be verified by the successive developments inside the encircled sections of Figure 9A through 10D. Again, the displaced hydrates would be hindered by the existing excess free water. In addition, some of dissolved CO_2 would be available to mix with the released methane. The thermodynamic conditions are favourable to allow both the CH_4 and CO_2 gas molecules to enclathrate in the hydrogen-bonded network of water molecules. After 89 hours, the reformation of the hydrates of mixed gases occurred. Translucent bubbles, which appeared after 45 hours (see figure 9B), existed even after further 44 hours (see figure 9D). This further extends the interest in idea of the replacement of methane by the CO_2 injection into methane hydrate reservoir to recover methane energy, ultimately permanent CO_2 sequestration through clathrate hydrate formation and consequently maintain the stability of the hydrate-rich sediments.

Key objective of the second micromodel experiment was to study the profound effect the LuviCap, the kinetic inhibitor, may have on the methane hydrate-water system after carbon dioxide is injected, and overall on the CO_2 driven methane displacement in the hydrates under the excess water conditions.

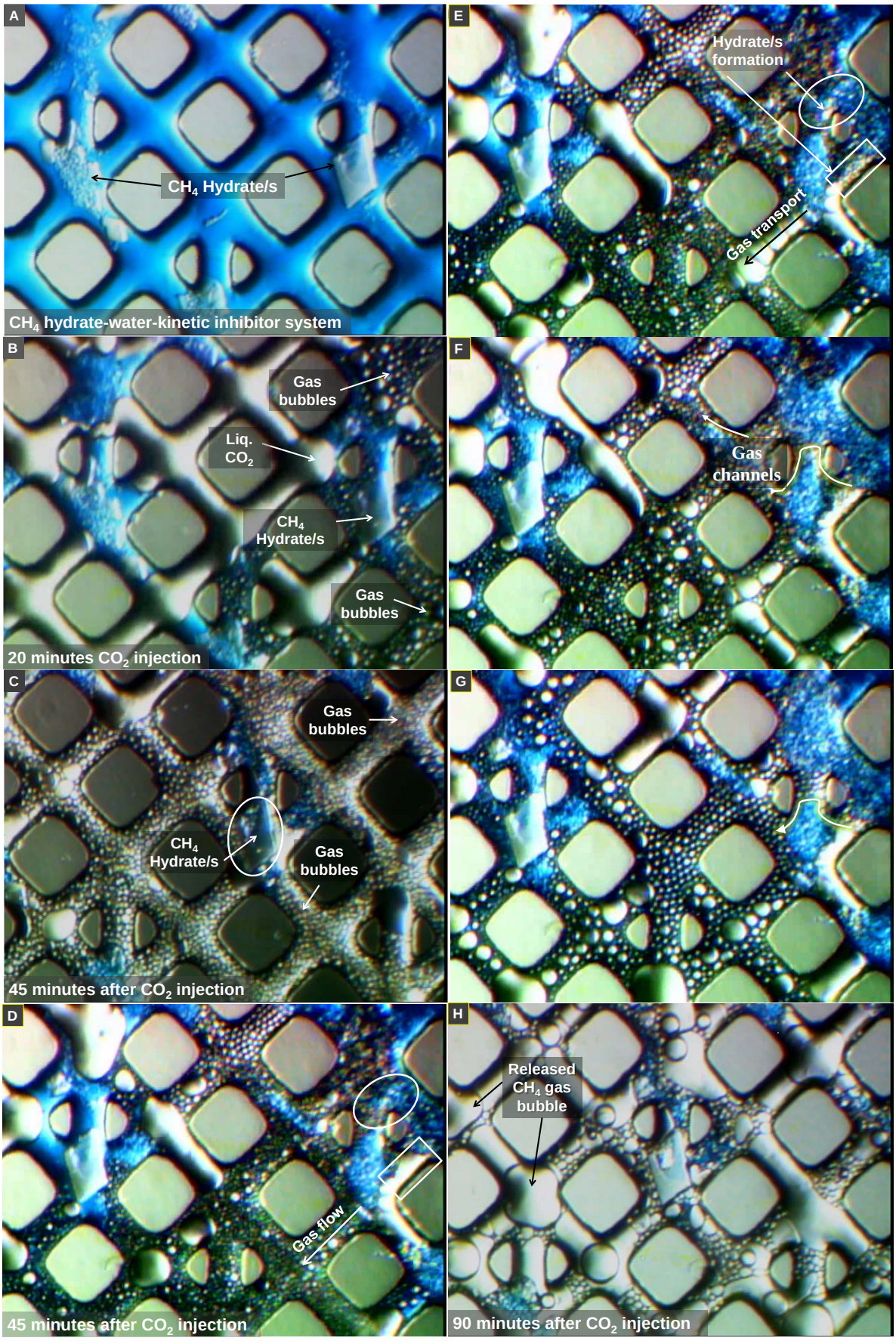

Figure 10: Visual 2D Micromodel section depicting the released methane bubble transport during the liquid CO_2 injection, subsequent hydrate (CO_2 or mixed CO_2-CH_4) formation and stabilized larger methane gas bubbles after 90 minutes.

In the second test, LuviCap was injected in the methane hydrate-water system (Figure 10A) before the introduction of liquid CO_2 at the thermodynamic conditions within both the CH_4 and CO_2 HSZ (276 K, HSZ-II). Morphological changes occurring in a prominent section of micromodel are presented in the Figure 10A through H. Within the 20 minutes of the liquid CO_2 injection in the methane hydrate-water-LuviCap system (Figure 10A), this micromodel section showed a 'bubbling phenomenon', that is gas bubbles being transported to this site (figure 10B). This indicates that the injected kinetic inhibitor (before CO_2 injection) could not have distributed evenly throughout the micromodel giving rise to the formation of CO_2 hydrate crystals (tiny) at those uncontacted sites. It could have led to the generation of heat of CO_2 hydrate formation, which is sufficient to weaken hydrogen-bonded network (host lattice) of CH_4 hydrates in its vicinity. Figure 10C depicts that the diamond shaped methane hydrate crystal also becomes translucent after 45 minutes of CO2 injection indicating the host lattice has been de-stabilized and some of the methane gas could have been released. However, later it regained its shape (see Figure 10D) indicating that cavities could have been reoccupied by the CO_2 or mixed CH_4-CO_2 gas. At this stage, hydrates begin to form at the sites where they were not existed before CO_2 injection (as shown in oval and square-shaped indicators of Figure 10C) and inflow of gas bubbles diminished. 90 minutes after CO_2 injection, the micromodel section showed the presence of methane gas in the form of bubbles interfacing with the liquid CO_2. Incoming bubbles might have transported the inhibitor from other sites and hence might have delayed hydrate formation. At this stage hydrates begin to form at the sites where they were not existed before CO_2 injection (as shown in oval and square shaped indicators of Figure 10E) and inflow of gas bubbles diminished. Although hydrates were formed, gas continues to enter in this region through the channels (see Figure 10F). Hydrates further continue to grow with the reduction in the entering gas bubbles. Figure 10D through Figure 10G clearly demonstrated the transportation of the gaseous molecules, liquid CO_2, CO_2 or mixed CH_4-CO_2 hydrate formation and the indirect indication of CH_4 replacement by the injected liquid CO_2. Further convection and diffusion through the so formed hydrate layers/films continued that resulted in the release of methane gas in the form of bubbles

interfacing with the liquid CO_2 after 90 minutes after CO_2 injection (refer to Figure 10H). The incoming bubbles might have transported the inhibitor from other sites and hence might have delayed hydrate formation. Temperature and pressure conditions are such that CO_2 would remain in liquid state and methane exists in gaseous state. Hence the bubbles seen in the figure 10H are of CH_4 gas.

3.2.1 Discussion of the results

In terms of practical application of this process, CO_2 sequestration under the HSZ-I and HSZ-III will face operational issues. Injected CO_2 will form CO_2-hydrates around the wellbore in the field test in relatively short time, as thermodynamic conditions fall in HSZ of either of CH_4 or CO_2 hydrates, thus creating the CO_2 injectivity issues. This will also reduce or completely prevent further advance of CO_2 away from wellbore (thus CO2 relative permeability), due to the reduction in the permeability of the hydrate porous medium and further contact methane hydrates for the possible CH_4-CO_2 replacement and the subsequent methane recovery. From operational practical point of view, the HSZ-II (i.e., inside methane HSZ and outside CO_2 HSZ) seems to be an optimum choice for integration of methane recovery and CO_2 storage in marine sediments. CO_2 replaces CH_4 in the hydrates to form methane hydrates. Moreover, CO_2 can also form the mixed CO_2-CH_4 hydrates for the injected CO_2 concentration up to 30% especially in HSZ-II (see Figure 1), specifically for the experimental pressure and temperature conditions in this study.

Table 2: Summary of the methane recovered through the CO_2-CH_4 replacement in hydrates.

Test	Temp--erature	Pressure	Methane recovered through CO2-CH4 replacement								
	(K)	(MPa)		Stage-1			Stage-2			Average	
			Initial (mol%)	Final (mol%)	Rate (mol%/day)	Recovery (%)	Final (mol%)	Rate (mol%/day)	Recovery (%)	Rate (mol%/day)	Recovery (%)
1	275.2	3.6	30.33	34.9	1.23	13.1	38.3	0.42	8.9	0.68	20.8
2	284	8.4	5.13	9.47	1.45	45.8	17.68	2.46	46.4	1.98	71.0
3	283.4	8.4	1.29	2.14	0.17	39.7	3.37	0.18	36.5	0.17	61.7
4	275.8	8.5	2.8	4.5	0.59	37.8	5.8	0.09	22.4	0.17	51.7

In our experimental work on the modified production/CO_2 sequestration rig, methane recoveries from the CO_2-CH_4 replacement in gas hydrates are summarized in Table-2. Rates and percentage recoveries are reported in two stages for comparison of the CO_2-CH_4 replacement. In Test-

1, first 89 hours recovered 13.1% methane at the rate of 1.23 mol%/day in stage-1, which slowed down to 0.42 mol%/day with lower methane recovery of 8.9% in the next 193 hours. Comparatively, the CO2-CH4 replacement rate in the Test-2 was 1.45 and 2.46 mol%/day with the 45.8% and 46.4% overall methane recovery (nearly same) in 72 (stage-1) and 80 hours (stage-2), respectively. Test-3 reported nearly same recovery rates (0.17 and 0.18 mol%/day in stage-1 and stage-2 respectively) and slightly lower recoveries in the stage-2 (36.5% in 120) compared to 39.7% in the stage -1 (188 hours). Note that both the Test-2 (Excess gas 74.8%) and Test-3 (comparatively higher water saturation of 26.7%) were conducted in HSZ-II (see Figure 1). Highest methane recovery of 71% was obtained in Test 2 at the experimental thermodynamic conditions existed in the HSZ-II (3.4% water saturation, 283.4 K and 8.4 MPa). CO_2 sequestration rate was also highest possibly owing to two factors: first the CO_2 dissolution in the water and then convective transport to the methane hydrates to incur CO_2-CH_4 replacement reaction; Secondly either the CH_4 hydrates or CH_4-CO_2 hydrates are formed for the long-term storage of CO_2 as hydrates (see Figure 10). When the test conditions were inside both the methane (just) and CO_2 HSZ at same pressure under higher water saturation of 26.7 mol% (Test-3), methane recovery from CO_2 replacement diminished by 9.3%. Both tests represent the oceanic methane hydrate conditions extends the wide range of depths at higher temperatures.

To find solution for CO_2 hydrate formation near the wellbore, the LuviCap (LDHI) was injected in Test-4 to delay the CO_2 hydrate formation. It was conducted at the same pressure, but at 275.8 K inside the HSZ-I. Test-4 yielded 37.8 and 22.4 methane recovery in 69 and 356 hours, respectively. About 20% drop in the overall methane recovery was observed in comparison with the Test-2. However, the methane recovery is comparably higher (51.7%) signifying the successful application of a kinetic inhibitor in the CO_2-CH_4 replacement process especially deep inside the CH_4 HSZ, representing the permafrost hydrate reservoirs. Results thus have pointed out that the CO_2 injection alone may not be enough for the CH_4-CO_2 replacement, so an effective methane recovery, and should be combined with the other production methods (such as inhibitor injection or depressurization).

Table 3: The amount of CO_2 captured in hydrates.

Test	Temperature	CO_2 in vapour (mol%)		CO_2 sequestered in hydrates	
	(K)	Initial	Final	(mol%)	(%)
1	275.2	69.67	61.70	7.97	11.4
2	284.0	94.87	82.32	12.55	13.2
3	283.4	98.71	96.63	2.08	2.10
4	275.8	97.20	94.20	30	3.10

CO2 dissolution in water is small and negligible compared to inclusion in gas hydrates

Potential of the CO_2 injection method was also evaluated in combination with the CO_2 sequestration and storage in the oceanic and permafrost methane hydrate reservoirs. Initial CO_2 content was measured in the vapour phase after completion of purging the remaining methane and the final CO_2 content was measured at the end of the experiment. The amount of the CO_2 captured is tabulated in Table-3. 13.2 % of CO2 was stored as hydrates in Test-2 (HSZ-II, the oceanic environment), whereas the Test-2 inside the HSZ-I successfully stored 11.4 mol% of CO_2 as hydrates in porous media. Although the Test-3 and Test-4 (HSZ-I) resulted in the lower CO_2 storage, these experimental results proved that the CO_2 sequestration in the CH_4 hydrate reservoirs yields the cost offsetting of the CO_2 injection operations through the methane recovery from CH_4-CO_2 replacement in hydrates and the simultaneous long term permanent subsurface CO_2 storage as hydrates.

Microscale experiments on the visual micromodel were conducted in both the HSZs I and II to mimic both the permafrost and oceanic hydrate conditions. Micromodel images under the HSZ-II in the first experiment clearly pointed out the potential of subsurface CO_2 storage as clathrate hydrate with CO_2 or CO_2-CH_4 hydrates. On the other hand, the second micromodel test revealed for the first time ever, the visual evidence of methane gas release from hydrates through its replacement by the injected liquid CO_2 while inferring the role of Luvicap in the replacement process.

4. CONCLUSIONS

CO_2 sequestration and storage into methane (CH_4) hydrate sediments were evaluated using two experimental setups: the modified production/CO_2 sequestration rig and a visual glass

micromodel. These experiments conducted at both the macro and microscale within the methane hydrate stability zone (HSZ) and within (HSZ-I)/outside the CO_2 HSZ (HSZ-II). Microscale investigations of CH_4 replacement by CO_2 in hydrates carried out using the modified production/ CO_2 sequestration rig provided 51.7% to 71% methane recovery irrespective of the presence of the excess water or excess gas in the hydrate sediments when liquid CO_2 injected. The highest 71% CH_4 was recovered in macroscale excess gas experiments within the HSZ-II, whereas the excess water conditions diminished the CH_4 recovery by 9.3% when the temperature is shifted just inside the CO2 HSZ at the same pressure. Deep inside the HSZ-I, a significant CH_4 production of 51.7% was obtained (permafrost) with an inhibitor application. These results concluded that the presence of excess water diminishes the methane recovery irrespective of higher hydrate saturation. Moreover, our results thus have pointed out that the CO_2 injection alone may not be enough for the CH_4-CO_2 replacement, so an effective methane recovery, and should be combined with the other production methods (such as inhibitor injection or depressurization). Macroscale results were further validated using the microscale investigations on visual glass micromodel for the CH_4-replacement/CO_2 storage kinetics thereby deploying a commercial kinetic inhibitor. Our novel microscale micromodel evaluations clearly revealed, for the first time ever, the release of CH_4 gas through the convection, slow CO_2 diffusive mass transfer and the CO_2-CH_4 replacement (in hydrate) mechanisms. Moreover, this process benefits from the long-term permanent CO_2 sequestration and storage in the form of clathrate hydrates (first micromodel results) while offsetting the cost of its injection through the clean energy methane recovery.

5. ACKNOWLEDGEMENT

Authors gratefully acknowledge the financial support (2003-2005) received from the Scottish Higher Education Funding Council. Thanks to Mr Jim Pantling for construction and maintenance of the experimental equipment. Dr Jadhawar thanks the Institute of Petroleum Engineering and the

Centre for Gas Hydrate Research for financial support. Useful comments from Ross Anderson and Rod Burgass are also gratefully acknowledged.

6. REFERENCES

[1]. Sloan, J. E. D.; Koh, C. A., Clathrate Hydrates of Natural Gases. Third Edit ed.; CRC Press: 2007.

[2]. Ruppel, C. D.; Waite, W. F., Timescales and Processes of Methane Hydrate Formation and Breakdown, With Application to Geologic Systems. Journal of Geophysical Research: Solid Earth 2020, 125, (8), e2018JB016459.

[3]. Milkov, A. V., Global estimates of hydrate-bound gas in marine sediments: how much is really out there? Earth-Science Reviews 2004, 66, (3), 183-197.

[4]. Englezos, P., Extraction of methane hydrate energy by carbon dioxide injection-key challenges and a paradigm shift. Chinese Journal of Chemical Engineering 2019, 27, (9), 2044-2048.

[5]. Makogon, Y. F., Hydrates of Hydrocarbons. PennWell Books: Tulsa, Oklahoma, 1997.

[6]. Chandrasekharan Nair, V.; Gupta, P.; Sangwai, J. S., Natural Gas Production from a Marine Clayey Hydrate Reservoir Formed in Seawater Using Depressurization at Constant Pressure, Depressurization by Constant Rate Gas Release, Thermal Stimulation, and Their Implications for Real Field Applications. Energy & Fuels 2019, 33, (4), 3108-3122.

[7]. McGuire, P. L., Recovery of Gas from Hydrate Deposits Using Conventional Technology. In SPE Unconventional Gas Recovery Symposium, Society of Petroleum Engineers: Pittsburgh, Pennsylvania, 1982; p 15

[8]. Holder, G. D.; Angert, P. F.; John, V. T.; Yen, S., A Thermodynamic Evaluation of Thermal Recovery of Gas from Hydrates in the Earth. Journal of Petroleum Technology 1982, 34, (5), 1127-1132.

[9]. Kamath, V. A.; Godbole, S. P., Evaluation of hot-brine stimulation technique for gas production from natural gas hydrates. Journal of Petroleum Technology 1987, 39, (11), 1379-1388.

[10]. Chandrasekharan Nair, V.; Mech, D.; Gupta, P.; Sangwai, J. S., Polymer Flooding in Artificial Hydrate Bearing Sediments for Methane Gas Recovery. Energy & Fuels 2018, 32, (6), 6657-6668.

[11]. Yin, Z.; Linga, P., Methane hydrates: A future clean energy resource. Chinese Journal of Chemical Engineering 2019, 27, (9), 2026-2036.

[12]. Booth, J. S.; Winters, W. J.; Dillon, W. P. In Circumstantial evidence of gas hydrate and slope failure associations on the U.S. Atlantic continental margin, International Conference on Natural Gas Hydrates: , 1994; Sloan, E. D., Jr., ; Happel, J.; Hnatow, M. A., Eds. Annals of the New York Academy of Sciences: 1994.

[13]. Collett, T. S.; Dallimore, S. R. In Detailed analysis of gas hydrate induced drilling and production hazards, Proceeding of the 4th International Conference on Gas Hydrates, Yokohama, Japan, 19-23 May 2002: Yokohama, Japan, 2002.

[14]. Freij-Ayoub, R.; Tan, C.; Clennell, B.; Tohidi, B.; Yang, J., A wellbore stability model for hydrate bearing sediments. Journal of Petroleum Science and Engineering 2007, 57, (1), 209-220.

[15]. Rogers RE, Yevi. *Gas hydrate theory explains lake Nyos disaster*. In: Proceedings of The 2nd International Conference on Natural Gas Hydrates, Toulouse, 1996.

[16]. Dickens, G. R.; O'Neil, J. R.; Rea, D. K.; Owen, R. M., Dissociation of oceanic methane hydrate as a cause of the carbon isotope excursion at the end of the Paleocene. Paleoceanography 1995, 10, (6), 965-971.

[17]. Zheng, J.; Chong, Z. R.; Qureshi, M. F.; Linga, P., Carbon dioxide sequestration via hydrates: A potential pathway towards decarbonization. Energy & Fuels 2020.

[18]. Jadhawar, P. S.; Mohammadi, A. H.; Yang, J.; Tohidi, B., Subsurface Carbon Dioxide Storage through Clathrate Hydrate formation. In Advances in the Geological Storage of Carbon Dioxide, Lombardi, A.; Beaubien, S., Eds. Springer publications: Netherlands, 2006; Vol. 65, pp 111-126.

[19]. Boswell, R.; Schoderbek, D.; Collett, T. S.; Ohtsuki, S.; White, M.; Anderson, B. J., The Iġnik Sikumi Field Experiment, Alaska North Slope: Design, Operations, and Implications for CO2–CH4 Exchange in Gas Hydrate Reservoirs. Energy & Fuels 2017, 31, (1), 140-153.

[20]. Davidson DW. *Clathrate Hydrates.* In: Franks F, editor. Water: A Comprehensive Treatise. New York: Plenum Press, 1973. p.115-163.

[21]. Adisasmito S, Frank RJ, Sloan ED Jr. *Hydrates of Carbon-Dioxide and Methane Mixtures*. Journal of Chemical Engineering Data 1991; 36(1): 68-71.

[22]. Teng, H.; Yamasaki, A., Can CO2 hydrate deposited in the ocean always reach the seabed? Energy Conversion and Management 1998, 39, (10), 1045-1051.

[23]. Yoon, J.-H.; Yamamoto, Y.; Komai, T.; Haneda, H.; Kawamura, T., Rigorous approach to the prediction of the heat of dissociation of gas hydrates. . Industrial & Engineering Chemistry Research 2003, 42, (5), 1111-1114.

[24]. Handa, Y. P., Compositions, Enthalpies of Dissociation, and Heat-Capacities in the Range 85-K to 270-K for Clathrate Hydrates of Methane, Ethane, and Propane, and Enthalpy of Dissociation of Isobutane Hydrate, as Determined by a Heat-Flow Calorimeter. Journal of Chemical Thermodynamics 1986, 18, (10), 915-921

[25]. Hirohama S, Shimoyama Y, Wakabayashi A, Tatsuta S, Nishida N. *Conversion of CH_4-Hydrate to CO_2 - Hydrate in liquid CO_2.* Journal of Chemical Engineering of Japan 1996; 29(6): 1014-1020.

[26]. Sivaraman R. *The potential role of hydrate Technology in sequestering Carbon Dioxide.* Gas TIPS. Fall 2003. http://www.gastechnology.org/

[27]. Ota, M.; Morohashi, K.; Abe, Y.; Watanabe, M.; Smith, J. R. L.; Inomata, H., Replacement of CH4 in the hydrate by use of liquid CO2. Energy Conversion and Management 2005, 46, (11), 1680-1691.

[28]. Ota, M.; Abe, Y.; Watanabe, M.; Smith, R. L.; Inomata, H., Methane recovery from methane hydrate using pressurized CO2. Fluid Phase Equilibria 2005, 228-229, 553-559.

[29]. Ohgaki K, Takano K, Sangawa H, Matsubara T, Nakano S. *Methane Exploitation by Carbon Dioxide from Gas Hydrates- Phase Equilibria for CO_2 - CH_4 mixed hydrate system.* Journal of Chemical Engineering of Japan, 1996; 29(3): 478-483.

[30]. KOMAI, T.; YAMAMOTO, Y.; OHGA, K., Dynamics of Reformation and Replacement of CO2 and CH4 Gas Hydrates. Annals of the New York Academy of Sciences 2000, 912, (1), 272-280.

[31]. Mahabadian, M. A.; Chapoy, A.; Burgass, R.; Tohidi, B., Development of a multiphase flash in presence of hydrates: Experimental measurements and validation with the CPA equation of state. Fluid Phase Equilibria 2016, 414, (0), 117-132.

[32]. Chapoy, A.; Burgass, R.; Tohidi, B.; Alsiyabi, I., Hydrate and Phase Behavior Modeling in CO 2 -Rich Pipelines. Journal of Chemical & Engineering Data 2015, 60, (2), 447-453.

[33]. Haghighi, H.; Chapoy, A.; Tohidi, B., Methane and Water Phase Equilibria in the Presence of Single and Mixed Electrolyte Solutions Using the Cubic-Plus-Association Equation of State. Oil & Gas Science and Technology - Rev. IFP 2009, 64, (2), 141-154.

[34]. Ohgaki, K.; Inoue, Y., A Proposal for Gas Storage on the Bottom of the Ocean, using Gas Hydrates. International Chemical Engineering 1994, 34, (3), 417-419.

[35]. Uchida T, Takeya S, Ebinuma T, Narita H. Replacing Methane with CO2 in clathrate hydrate: Observations using Raman Spectroscopy. Greenhouse Gas Control Technologies, East Melbourne. 2001. 523-527.

[36]. Komai T; Kawabe Y; Kawamura T; J., Y., Extraction of Gas Hydrates using CO2 sequestration. In International Offshore and Polar Engineering Conference, Hawaii USA, 2003.

[37]. Ota, M.; Abe, Y.; Watanabe, M.; Smith, R. L.; Inomata, H., Methane recovery from methane hydrate using pressurized CO2. Fluid Phase Equilibria 2005, 228-229, 553-559.

[38]. Yoon JH; Kawamura T; Yamamoto Y; T., K., Transformation of methane hydrate to carbon dioxide hydrate: in situ Raman spectroscopic observations. J Phys Chem A 2004, 108, 5057–9.

[39]. Lee, H., Seo, Y., Seo, Y.T., Moudrakovski, I.L., Ripmeester, J.A., *Recovering methane from solid methane hydrate with carbon dioxide*, Angewandte Chemie-International Edition; 2003, 42(41):5048-5051.

[40]. McGrail BP, Zhu T, Hunter RB, White MD, Patil SL, Kulkarni AS. *A New Method for Enhanced Production of Gas hydrates with CO_2.* In: Gas Hydrates: Energy Resource Potential and Associated Geologic Hazards, AAPG Hedberg conference, Vancouver, 2004.

[41]. Lee, B. R.; Koh, C. A.; Sum, A. K., Quantitative measurement and mechanisms for CH4 production from hydrates with the injection of liquid CO2. Physical Chemistry Chemical Physics 2014, 16, (28), 14922-14927.

[42]. Ersland, G.; Husebø, J.; Graue, A.; Baldwin, B. A.; Howard, J.; Stevens, J., Measuring gas hydrate formation and exchange with CO2 in Bentheim sandstone using MRI tomography. Chemical Engineering Journal 2010, 158, (1), 25-31.

[43]. Parshall, J., Production Method for Methane Hydrate Sees Scientific Success. Journal of Petroleum Technology 2012, 64, (08), 50-51.

[44]. Yuan, Q.; Sun, C.-Y.; Liu, B.; Wang, X.; Ma, Z.-W.; Ma, Q.-L.; Yang, L.-Y.; Chen, G.-J.; Li, Q.-P.; Li, S.; Zhang, K., Methane recovery from natural gas hydrate in porous sediment using pressurized liquid CO2. Energy Conversion and Management 2013, 67, 257-264.

[45]. Tohidi B, Anderson R, Clennell B, Burgass RW, Biderkab AB. *Visual Observation of Gas Hydrate Formation and Dissociation in Synthetic Porous Media by Means of Glass Micromodels.* Geology, 2001, **29(9)**, 867–870.

[46]. Anderson R, Biderkab AB, Tohidi B., Clennell MB. *Visual Observation of Gas Hydrate Formation In Glass Micromodels.* EAGE 63rd Conference & Technical Exhibition — Amsterdam, The Netherlands, 2001.

[47]. Jang, J. Gas Production from Hydrate-Bearing Sediments. Georgia Institute of Technology, 2011.

[48]. Pandey, J. S.; Solms, N. V., Hydrate Stability and Methane Recovery from Gas Hydrate through CH4–CO2 Replacement in Different Mass Transfer Scenarios. Energies 2019, 12, (2309).

[49]. Okwananke, A.; Hassanpouryouzband, A.; Vasheghani Farahani, M.; Yang, J.; Tohidi, B.; Chuvilin, E.; Istomin, V.; Bukhanov, B., Methane recovery from gas hydrate-bearing sediments: An experimental study on the gas permeation characteristics under varying pressure. Journal of Petroleum Science and Engineering 2019, 180, 435-444

[50]. Nakano, S.; Ohgaki, K., Relative cage-occupancy of CO2-methane mixed hydrate, . Journal of Chemical Engineering of Japan 2000, 33, (3).

[51]. Sloan ED Jr. *Fundamental Principles and Applications of Natural Gas Hydrates.* Nature 2003; 426:353-359.

[52]. Demurov, A.; Radhakrishnan, R.; Trout, B. L., Computations of diffusivities in ice and CO2 clathrate hydrates via molecular dynamics and Monte Carlo simulations. The Journal of Chemical Physics 2002, 116, (2), 702-709.

“TOC Graphic”

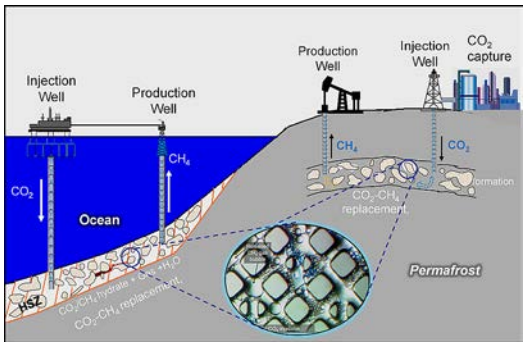

We would like to confirm that all text are legible within the instructed size of 8.25 cm x 4.45 cm (300 dpi).